

# Planarity of Acetamides, Thioacetamides, and Selenoacetamides: Crystal Structure of *N,N*-Dimethylselenoacetamide

Shuqiang Niu,<sup>1</sup> Guang Ming Li,<sup>2</sup> Ralph A. Zingaro,<sup>3</sup> Joseph H. Reibenspies,<sup>3</sup> and Toshiko Ichiye<sup>1</sup>

<sup>1</sup>*School of Molecular Biosciences, Washington State University, Pullman, Washington 99164-4660*

<sup>2</sup>*Product Development Department, Cosmetics Division, Tokiwa Corporation, Keitoku Building 5F, 1-9-5 Oji, Kita-Ku, Tokyo 114-0002, Japan*

<sup>3</sup>*Department of Chemistry, Texas A&M University, College Station, Texas 77843-3255*

Received 29 November 2000

**ABSTRACT:** The planarity of acetamides **1a–3a**, thioacetamides **4a–6a**, and selenoacetamides **7a–9a**,  $R^1R^2NC(=E)CH_3$  where  $E = O, S, Se$ , and  $R^1, R^2 = H$  or  $CH_3$ , was investigated using theoretical calculations at the density functional theory (DFT) level. The calculations showed that the methyl substitution on nitrogen and the change from the amide moiety ( $NC=O$ ) to  $NC=S$  or  $NC=Se$  group increased the double bond character of the  $N-C$  bond. In other words, the planarity of these compounds (**1a–9a**) increases in the order  $NH_2 < NHCH_3 < N(CH_3)_2$  and  $O < S < Se$ . The calculations of bending energy suggest that the planar geometry represents the lowest energy conformation for all compounds investigated in this work. *N,N*-Dimethyl-selenoacetamide (**9a**),  $(CH_3)_2NC(Se)CH_3$ , has the largest bending energy of 10.37 kcal/mol, which suggests that it possesses the greatest planarity among the compounds **1a–9a**. However, the solid phase molecular structure of **9a** was found to be slightly nonplanar by X-ray crystallography. The slight nonplanarity observed experimentally

is very likely the consequence of intermolecular interactions arising within the crystal packing. © 2002 Wiley Periodicals, Inc. Heteroatom Chem 13:380–386, 2002; Published online in Wiley InterScience (www.interscience.wiley.com). DOI 10.1002/hc.10056

## INTRODUCTION

The conformations of a polypeptide chain have been well recognized as arising from the geometrical properties of a linked sequence of peptide groups. Generally, peptide groups are considered to have a rigid, planar structure with a trans conformation in 3D analysis as a consequence of resonance interactions (Scheme 1) [1]. The peptide bond (the amide C–N bond) has partial double bond character due to a lone-pair electron density which the nitrogen atom donates to the C=O  $\pi$  antibonding orbital. The knowledge and understanding of the relationships between the  $\alpha$ -carbon and the peptide bond as well as between the C=O bond and the peptide bond are necessary to comprehend biochemical and biophysical roles of proteins.

In a recent study on the rubredoxin model compounds  $[Fe\{SCH_2CON(CH_3)_2\}_4]^{2-}$  and  $[Fe(SCH_2CONH_2)_4]^{2-}$  [2], Walters and co-workers investigated hydrogen bonding and charge–dipole effects of the *N,N*-dimethylacetamide and acetamide groups on

Correspondence to: Ralph A. Zingaro; e-mail: zingaro@mail.chem.tamu.edu.

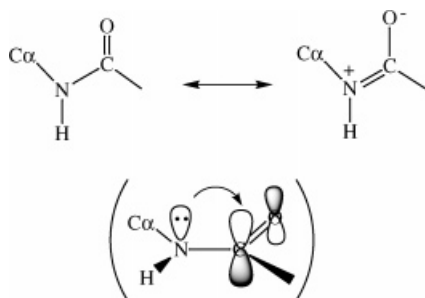
Contract grant sponsor: Robert A. Welch Foundation, Texas.

Contract grant sponsor: National Institute of Health.

Contract grant number: GM45303.

Contract grant sponsor: Selenium–Tellurium Development Association.

© 2002 Wiley Periodicals, Inc.



SCHEME 1

the redox center. It appears that the redox potential is strongly influenced by polar amide groups adjacent to the metal–ligand redox center, which leads to a relatively positive reduction potential shift (390 mV) with respect to  $[\text{Fe}(\text{SC}_2\text{H}_5)_4]^{2-}$  in the same solution ( $\text{CH}_3\text{CN}$ ). Clearly, the changes of the structural and electronic properties of amide groups near the redox site have significant influence on the reduction potential of the electron transfer proteins through hydrogen bonding and the charge–dipole interaction. Thus, understanding how the internal factors contribute to the peptide bond properties is essential in studying perturbative interaction of the redox site with the environment. Structural characteristics of the amide C–N bond have been studied experimentally and/or theoretically on some smaller amide compounds with primary interest in the planarity or nonplanarity of the bonds around nitrogen [3–13]. For example, a planar structure was strongly suggested for formamide,  $\text{H}_2\text{NC}(\text{O})\text{H}$ , by gas electron diffraction (GED), microwave spectroscopy (MW), and high-level calculations [3–7]. However, a neutron diffraction (ND) investigation of acetamide,  $\text{H}_2\text{NC}(\text{O})\text{CH}_3$ , showed a nonplanar orientation around the nitrogen [8]. Recently, Mack and Oberhammer investigated the planarity of *N,N*-dimethylacetamide (DMA),  $(\text{CH}_3)_2\text{NC}(\text{O})\text{CH}_3$ , by GED analysis and theoretical calculations [13]. Although no clear-cut answer was obtained, the planar geometry was suggested as having the lowest energy conformation for this compound (DMA).

In this work, theoretical calculations at the DFT level have been performed to investigate the planarity of a series of acetamides and their sulfur and selenium analogs (thioacetamides and selenoacetamides): **1a–9a**,  $\text{R}^1\text{R}^2\text{NC}(\text{E})\text{CH}_3$  where  $\text{R}^1, \text{R}^2 = \text{H}$  or  $\text{CH}_3$  and  $\text{E} = \text{O}, \text{S}, \text{Se}$ , as well as the relationship between the structure and electronic property. Also, the structure of *N,N*-dimethyl-selenoacetamide (**9a**) has been characterized by single crystal X-ray diffraction.

## EXPERIMENTAL SECTION

### Computational Details

The geometries have been optimized using density functional theory (DFT) [14], specifically, utilizing the Becke three-parameter hybrid exchange functional [15–17] and the Lee–Yang–Parr correlation functional [18] (B3LYP). The triple- $\zeta$  basis sets 6-311G with polarization functions (6-311G\*\*) were used for nitrogen, carbon, hydrogen, oxygen, sulfur, and selenium atoms. The nonplanar structures are described by the fixed nitrogen as an  $\text{sp}^3$  hybrid center. Full natural bond orbital (NBO) analysis was carried out on charge, orbital energy, second-order perturbative energy, and dipole moment calculations at the MP2/6-311G\*\* level using the DFT geometry (MP2//DFT/6-311G\*\*). All DFT and MP2 calculations were performed with GAUSSIAN 98 [19] in SGI and IBM workstations in the group.

### Crystal Structure Determination of *N,N*-Dimethyl-selenoacetamide (**9a**)

Compound **9a** was synthesized according to the previously reported procedure [20]. X-ray-quality crystals of **9a** were prepared by recrystallization from hexane- $\text{CH}_2\text{Cl}_2$  solution under refrigeration. A yellow plate of **9a** was mounted on a glass fiber at room temperature. Preliminary examination and data collection were performed on a Siemens P4 single crystal diffractometer (oriented graphite monochromator; Mo  $\text{K}\alpha$  radiation) at 193 (2) K. Cell parameters were calculated from the least-squares fitting for high-angle reflections ( $2\theta > 15^\circ$ ). Omega ( $\omega$ ) scans for several intense reflections indicated acceptable crystal quality. Data were collected from  $6.78$  to  $49.98^\circ$  ( $2\theta$ ), and scan width for data collection was  $2.0^\circ$  in  $\omega$ , with a variable scan rate between  $3.0$  and  $15.0^\circ/\text{min}$ . The three standards, collected every three reflections, showed no significant trends. Background measurements using stationary crystal and stationary counter technique were made at the beginning and the end of each scan for half the total scan time.

Lorentz and polarization corrections were applied to 1085 reflections. A semiempirical absorption correction was applied. A total of 1025 reflections ( $R_{\text{int}} = 0.034$ ) were used in the calculation of  $R(F)$ . The structure was solved by direct methods [21] and refined using a full-matrix least-squares anisotropic refinement for all non-hydrogen atoms [22]. Hydrogen atoms were placed in idealized positions with isotropic thermal parameters riding on the attached atom. Neutral atom scattering factors and anomalous scattering factors were taken from the literature

[23]. Crystal structure parameters are given in Table 1, and the atomic coordinates and isotropic thermal parameters for non-hydrogen atoms are given in Supplementary Data.

The structure was refined with a merohedral twinning component (inversion twin law). A ratio of 39:61 of twin components was observed. A semiempirical psi scan correction was applied to the data and the structure was refined to 5.9% (*RF*).

## RESULTS AND DISCUSSION

### Calculations

DFT calculations were performed on acetamides **1a–3a**, thioacetamides **4a–6a**, and selenoacetamides **7a–9a**,  $R^1R^2NC(=E)CH_3$  where  $E = O, S, Se$  and  $R^1, R^2 = H$  or  $CH_3$ , in order to understand their geometric properties and bonding character. The DFT fully

optimized stationary points of **1a–9a** are shown in Fig. 1.

The DFT equilibrium geometries of compounds **1a–9a** favor a planar structure at the B3LYP/6-311G\*\* level. The sum of the bond angles around nitrogen  $\alpha_N$  is approximately  $360^\circ$  for all compounds. In comparison to the GED rigid geometry [13], the DFT optimized C(1)=O and N–C(1) bonds of **3a** are slightly shorter by  $0.005^\circ$  and longer by  $0.008 \text{ \AA}$ , respectively. In comparison to the X-ray experimental results (see crystal structure of **9a** in the next section), the DFT optimized C(1)=Se and N–C(1) bonds of **9a** are shorter by  $0.034$  and  $0.010 \text{ \AA}$ , respectively. Overall, the calculated geometric parameters of **3a** and **9a** are in good agreement with those observed experimentally.

The DFT equilibrium geometries were compared to determine the effects of methyl substitutions. In the first methyl substitution on the nitrogen atom, only slight changes occurred (**1a–2a**) in the C(1)=O ( $+0.004 \text{ \AA}$ , N–C(1) ( $0.000 \text{ \AA}$ ), C(1)–C(2) ( $0.000 \text{ \AA}$ ) bond distances, and N–C(1)–C(2) bond angle ( $-0.3^\circ$ ). However, with the second methyl substitution, the C(1)=O, N=C(1), C(1)–C(2) bonds, and the N–C(1)–C(2) bond angle of **3a** obviously increased by  $0.006, 0.009, 0.003 \text{ \AA}$ , and  $2.1^\circ$  with respect to **1a**, respectively. Similarly, with the increase in methyl substitution for thioacetamides from **4a** through **5a** to **6a**, the C(1)=S and C(1)–C(2) the bonds get longer. However, the N–C(1) bond and the N–C(1)–C(2) bond angle differ from the above tendency. The first methyl substitution in **5a** leads to a slight decrease in the N–C(1) bond distance and the N–C(1)–C(2) bond angle with respect to **4a**, whereas the second methyl substitution in **6a** leads to a clear increase in the N–C(1) bond distance and the N–C(1)C(2) bond angle. A similar tendency is demonstrated for selenoacetamides from **7a** through **8a** to **9a** for the change of the C(1)=Se, N–C(1), C(1)–C(2) bonds, and the N–C(1)–C(2) bond angle. It appears that the methyl substitutions decrease the double bond character of the C(1)–E ( $E = O, S, Se$ ) because of the electronic effect of the methyl group. Generally, the double bond character of the N–C(1) should be increased with increasing the number of methyl substitutions. The oscillation of the N–C(1) bond length ( $NHCH_3 < NH_2 < N(CH_3)_2$ ) and the bending of the N–C(1)–C(2) bond angle indicates that the steric effect of methyl substitutions may lead to a decrease in the strength of N–C(1) bond.

The DFT equilibrium geometries were also compared to determine the effects of substitution of the carbonyl oxygen with sulfur or selenium. Comparing **1a, 4a**, and **7a**, the bond distances of the N–C(1) and

TABLE 1 Crystal Data and Structure Refinement

Identification code	rz44
Empirical formula	$C_8H_{18}N_2Se_2$
Formula weight	300.16
Temperature	193 (2) K
Wavelength	0.71073 $\text{\AA}$
Crystal system	Monoclinic
Space group	<i>Cc</i>
Unit cell dimensions	$a = 9.776(5) \text{ \AA}$ $\alpha = 90.000(5)^\circ$ $b = 7.762(5) \text{ \AA}$ $\beta = 104.230(5)^\circ$ $c = 8.219(5) \text{ \AA}$ $\gamma = 90.000(5)^\circ$
Volume	$604.5 (6) \text{ \AA}^3$
Z	2
Density (calculated)	$1.649 \text{ mg/m}^3$
Absorption coefficient	$6.075 \text{ mm}^{-1}$
<i>F</i> (000)	296
Crystal size/mm	$0.60 \times 0.40 \times 0.20$
$\theta$ Range for data collection	$3.39$ to $24.99^\circ$
Index ranges	$-11 \leq h \leq 11$ , $-9 \leq k \leq 9$ , $-9 \leq l \leq 9$
Reflections collected	1032
Independent reflections	982 [ $R_{int} = 0.0360$ ]
Completeness to $\theta = 24.99^\circ$	99.8%
Absorption correction	$T_{max} = 0.98$ $T_{min} = 0.96$
Refinement method	Full-matrix least-squares on $F^2$
Data/restraints/parameters	982/2/56
Goodness-of-fit on $F^2$	1.036
Final <i>R</i> indices [ $I > 2\sigma(I)$ ]	$R1 = 0.0592$ , $wR2 = 0.1459$
<i>R</i> indices (all data)	$R1 = 0.0728$ , $wR2 = 0.1571$
Absolute structure parameter	0.0 (3)
Largest diff. peak and hole	$0.409$ and $-0.483 \text{ e.\AA}^{-3}$

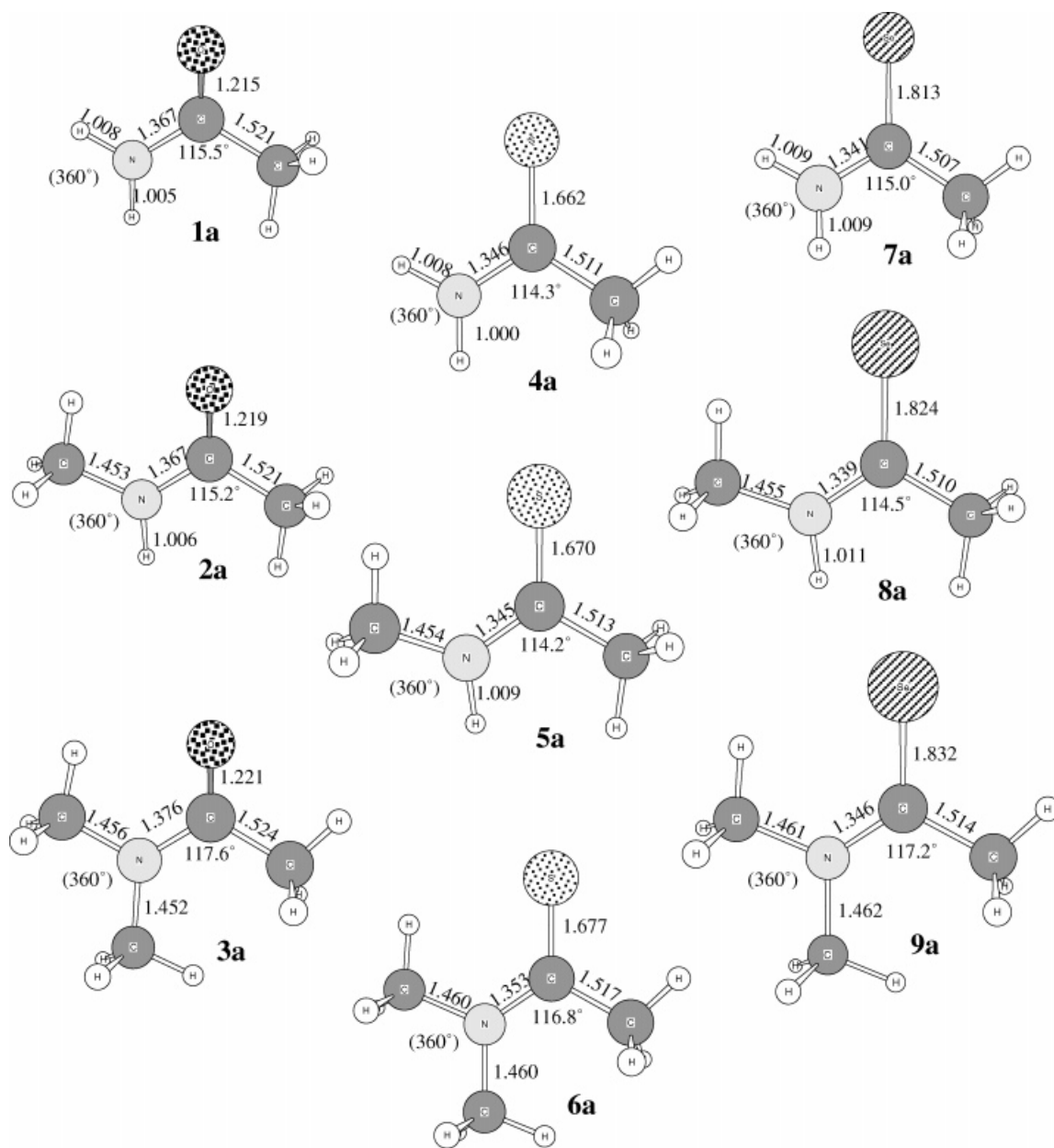


FIGURE 1 The B3LYP optimized geometrics of **1a–9a**.

C(1)–C(2) bonds decrease in the order  $O > S > Se$ . A similar tendency in the N–C(1) and C(1)–C(2) bonds occur in other methyl substituted compounds:  $2a > 5a > 8a$  and  $3a > 6a > 9a$ . Clearly, the atomic properties of the C=E group directly affects the properties of the N–C(1) bond.

To elucidate the relationship between the geometry and the electronic structure of compounds **1a–9a**, NBO analysis on charge, orbital energy, second-order perturbative energy (Table 2) was carried out. Generally, the N lone pair orbital ( $Lp_N$ ) is very sensitive to methyl substitutions, whereas the  $\pi_{C>E}$  and  $\pi_{C=E}^*$  orbitals are sensitive to the properties of

atoms E (E = O, S, Se). Methyl substitution leads to a higher-lying  $Lp_N$  orbital and increase donor ability of the lone pair electrons. As the  $\pi_{C>E}$  and  $Lp_N$  orbitals rise, the second-order perturbative energy arose from a donating interaction between the  $Lp_N$  and  $\pi_{C>E}^*$  orbitals obviously increases. Clearly, the lone pair electron density decreases and the electron density of the  $\pi_{C>E}^*$  orbital increases with the donor interaction. Thus, the N–C(1) double bond character is related to the properties of the  $\pi_{C>E}$  and  $Lp_N$  orbitals although the steric effect of the N,N-substitution may have influence on the donating interaction between the  $Lp_N$  and  $\pi_{C=E}^*$  orbitals.

**TABLE 2** NBO Analysis on Charge (e), Orbital Energy (a.u.), and Second-Order Perturbative Energy (kcal/mol) of **1a–9a** at MP2/B3LYP

Compounds	$\pi_{C=E}$			$Lp_N$		$\pi_{C=E}^*$			$Lp_N - \pi_{C=E}^*$
	$E$ (a.u.)	$q^C$	$q^E$	$E$ (a.u.)	$q^N$	$E$ (a.u.)	$q^C$	$q^E$	$\Delta E$ (2)
<b>1a</b>	-0.50851	0.508	1.487	-0.39198	1.811	0.22198	0.152	0.052	82.50
<b>2a</b>	-0.50050	0.496	1.500	-0.37363	1.773	0.21578	0.152	0.055	91.02
<b>3a</b>	-0.49704	0.502	1.490	-0.35973	1.748	0.21685	0.167	0.055	89.39
<b>4a</b>	-0.47074	0.647	1.309	-0.39825	1.740	0.14999	0.164	0.087	85.87
<b>5a</b>	-0.37373	0.496	1.496	-0.37875	1.687	0.07729	0.176	0.079	131.15
<b>6a</b>	-0.36840	0.501	1.484	-0.36436	1.664	0.07797	0.238	0.081	132.49
<b>7a</b>	-0.35727	0.491	1.488	-0.39914	1.715	0.05897	0.241	0.077	122.51
<b>8a</b>	-0.34139	0.435	1.558	-0.37986	1.663	0.05073	0.242	0.075	146.52
<b>9a</b>	-0.33609	0.441	1.545	-0.36517	1.640	0.05209	0.270	0.078	149.26

To further understand the planarity and bonding structure of compounds **1a–9a**, we have optimized their bent structures, **1b–9b**, where nitrogen is forced to be an  $sp^3$  hybrid center. The bending energies, total NBO dipole moment changes, and the bond length changes of N–C(1) and C=E between the bent (**1b–9b**) and planar (**1a–9a**) structures are shown in Table 3. The calculations show that (i) the amide group bending leads to a decrease in the C=E bond length ( $-0.003$  to  $-0.019$  Å) and an increase in the N–C(1) bond length ( $+0.031$  to  $+0.052$  Å); (ii) the total dipole moment change increases in the order of  $NH_2 < NHCH_3 < N(CH_3)_2$  and  $O < S < Se$ ; (iii) the bending energy increases in the order of  $NH_2 < NHCH_3 < N(CH_3)_2$  and  $O < S < Se$ ; and (iv) the planarity of the amide group is more sensitive to the methyl substitutions than the atomic property of E (the slopes of compound vs methyl substitution are 2.125, 2.940, and 3.270, whereas the slopes of compound vs E are 0.830, 1.935, and 1.975). Overall, *N,N*-dimethyl-selenoacetamide (**9a**) has the largest bending energy (10.37 kcal/mol) and the largest dipole moment change. Thus, the factors that contribute to the planarity of the amide group are the steric effects

**TABLE 3** The N–C and C=E Bond Distance Changes, Total NBO Dipole Moment Changes, and Bending Energy of Bent Structures of **1b–9b** relative to Planar Structures of **1a–9a**

Compounds	$\Delta r_{N-C}$ (Å)	$\Delta r_{C=E}$ (Å)	$\Delta D_{Total}$ (Debye)	$\Delta E$ (kcal/mol)
<b>1b</b>	+0.031	-0.003	-0.39	2.17
<b>2b</b>	+0.033	-0.006	-0.55	4.73
<b>3b</b>	+0.040	-0.006	-0.68	6.42
<b>4b</b>	+0.031	-0.008	-0.76	3.43
<b>5b</b>	+0.042	-0.015	-1.08	7.72
<b>6b</b>	+0.051	-0.018	-1.46	9.31
<b>7b</b>	+0.031	-0.009	-0.84	3.83
<b>8b</b>	+0.042	-0.017	-1.19	8.60
<b>9b</b>	+0.052	-0.019	-1.56	10.37

of the methyl substitution and the electronic effects of the methyl substitution and the E substitution.

### Crystal Structure of **9a**

The ORTEP drawing of *N,N*-dimethyl-selenoacetamide (**9a**) is presented in Fig. 2, and the selected bond distances and angles are listed in Table 4. The C–Se bond distance [(1.866 (19) Å) in **9a** is among the longest C–Se distances reported for selenoamides (including their metal complexes) [24–32] and selenoureas [33–35]. All bond angles around nitrogen and C(1) atoms are close to  $120^\circ$ . The sum of the nitrogen bond angles  $\alpha_N = 359.9^\circ$ , and the sum of bond angles around C(1) is exactly  $360.0^\circ$ . The torsion angles are  $C(4)-N(1)-C(1)-Se(1) = 177.9^\circ$ ,  $C(4)-N(1)-C(1)-C(2) = -1.0^\circ$ ,  $C(3)-N(1)-C(1)-Se(1) = 0.2^\circ$ ,  $C(3)-N(1)-C(1)-C(2) = -178.8^\circ$ . These results suggest a slightly nonplanar structure for compound **9a**. In addition, because selenium atom and methyl group have the

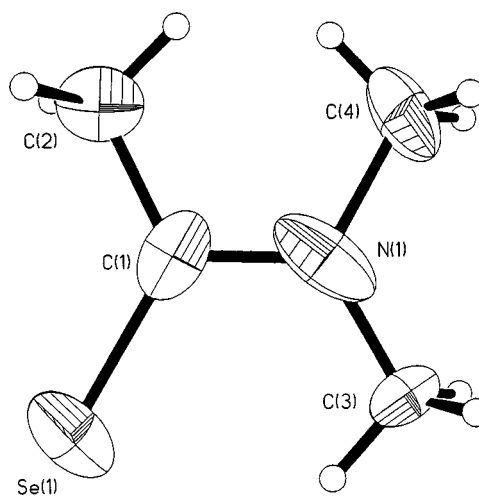
**FIGURE 2** Crystal structure of **9a**.

TABLE 4 Bond Lengths [Å] and Angles

Se(1)–C(1)	1.858 (14)
C(2)–C(1)	1.57 (2)
C(1)–N(1)	1.342 (13)
N(1)–C(4)	1.43 (3)
N(1)–C(3)	1.488 (18)
N(1)–C(1)–C(2)	116.4 (12)
N(1)–C(1)–Se(1)	119.9 (9)
C(2)–C(1)–Se(1)	123.7 (11)
C(1)–N(1)–C(4)	119.0 (11)
C(1)–N(1)–C(3)	119 (2)
C(4)–N(1)–C(3)	122 (2)

same value of van der Waals radius (2.00 Å) [36], this molecule can be seen to possess a plane of symmetry along the C(1)–N(1) bond. This is probably one of the reasons that *N,N*-dimethyl-selenoacetamide (**9a**) has a much higher melting point (78–80) than that (–20) of its oxygen analog **3a**.

### CONCLUDING REMARKS

Theoretical calculations show that, (i) both substitution of the amino hydrogen atoms by methyl groups and substitution of the amide carbonyl oxygen atom by sulfur and selenium lead to an increase of planarity for all compounds **1a–9a**; (ii) the planarity is more sensitive to methyl substitution than to the change of oxygen to sulfur and selenium; (iii) the bending energy and the total dipole moment change increases in the order  $\text{NH}_2 < \text{NHCH}_3 < \text{N}(\text{CH}_3)_2$  and  $\text{O} < \text{S} < \text{Se}$  and (iv) *N,N*-dimethyl-selenoacetamide (**9a**) has the largest bending energy of 10.37 kcal/mol and the largest dipole moment change. Consequently, a planar structure represents the lowest energy conformation for all compounds **1a–9a**. The slight nonplanarity of **9a** observed experimentally is very likely due to the intermolecular interactions within the crystal.

### SUPPLEMENTARY DATA

Supplementary data are available from the Cambridge Crystallographic Data Centre, 12 Union Road, Cambridge CB2 1EZ, UK on request. Listing of all bond distances and bond angles, anisotropic displacement parameters, hydrogen atom coordinates and isotropic displacement parameters (7 pages).

### REFERENCES

- [1] Bose, K.; Huang, J.; Haggerty, B. S.; Rheingold, A. L.; Salm, R. J.; Walters, M. A. *Inorg Chem* 1997, 36, 4596.
- [2] Chung, W. P.; Dewan, J. C.; Tuckerman, M.; Walters, M. A. *Inorg Chimica Acta* 1999, 291, 388.
- [3] Kitano, M.; Kuchitsu, K. *Bull Chem Soc, Jpn* 1974, 47, 67.
- [4] Kurland, R. J.; Wilson, E. B. *J Chem Phys* 1957, 27, 585.
- [5] Costain, C. C.; Dowling, J. M. *J Chem Phys* 1960, 32, 158.
- [6] Brown, R. D.; Godfrey, P. D.; Kleibomer, B. *J Mol Spectrosc* 1987, 124, 34.
- [7] Fogarasi, G.; Szalay, P. G. *J Phys Chem A* 1997, 101, 1400.
- [8] Jeffrey, G. A.; Ruble, J. R.; McMullan, R. K.; DeFrees, D. J.; Binkley, J. S.; Pople, J. A. *Acta Crystallogr Sect B* 1980, 36, 2292.
- [9] Kitano, M.; Kuchitsu, K. *Bull Chem Soc Jpn* 1973, 46, 3048.
- [10] Kitano, M.; Kuchitsu, K. *Bull Chem Soc Jpn* 1974, 47, 631.
- [11] Kitano, M.; Fukuyama, T.; Kuchitsu, K. *Bull Chem Soc Jpn* 1973, 46, 384.
- [12] Schultz, G.; Hargittai, I. *J Phys Chem* 1993, 97, 4966.
- [13] Mack, H.-G.; Oberhammer, H. *J Am Chem Soc* 1997, 119, 3567.
- [14] Parr, R. G.; Yang, W. *Density-Functional Theory of Atoms and Molecules*; Oxford University Press: Oxford, UK, 1989.
- [15] Becke, A. D. *Phys Rev* 1988, A38, 3098.
- [16] Becke, A. D. *J Chem Phys* 1993, 98, 1372.
- [17] Becke, A. D. *J Chem Phys* 1993, 98, 5648.
- [18] Lee, C.; Yang, W.; Parr, R. G. *Phys Rev* 1988, B37, 785.
- [19] Frisch, M. J.; Trucks, G. W.; Schlegel, H. B.; Scuseria, G. E.; Robb, M. A.; Cheeseman, J. R.; Zakrzewski, V. G.; Montgomery, J. A.; Stratmann, R. E.; Burant, J. C.; Dapprich, S.; Millam, J. M.; Daniels, A. D.; Kudin, K. N.; Strain, M. C.; Farkas, O.; Tomasi, J.; Barone, V.; Cossi, M.; Cammi, R.; Mennucci, B.; Pomelli, C.; Adamo, C.; Clifford, S.; Ochterski, J.; Petersson, G. A.; Ayala, P. Y.; Cui, Q.; Morokuma, K.; Malick, K. D.; Rabuck, A. D.; Raghavachari, K.; Foresman, J. B.; Cioslowski, J.; Ortiz, J. V.; Stefanov, B. B.; Liu, G.; Liashenko, A.; Piskorz, P.; Komaromi, I.; Gomperts, R.; Martin, R. L.; Fox, D. J.; Keith, T.; Al-Laham, M. A.; Peng, C. Y.; Nanayakkara, A.; Gonzalez, C.; Challacombe, M.; Gill, P. M. W.; Johnson, B. G.; Chen, W.; Wong, M. W.; Andres, J. L.; Head-Gordon, M.; Replogle, E. S.; Pople, J. A. *Gaussian 98, Revision A.6*, Gaussian Inc., Pittsburgh, PA, 1998.
- [20] Li, G. M.; Zingaro, R. A. *J Chem Soc, Perkin Trans* 1998, 1, 647.
- [21] Sheldrick, G. M. *SHELXS-86 Program for Crystal Structure Solution*; Institut für Anorganische Chemie der Universität, Tammanstrasse 4, D-3400 Gottingen, Germany, 1986.
- [22] Sheldrick, G. M. *SHELXS-93 Program for Crystal Structure Refinement*; Institut für Anorganische Chemie der Universität, Tammanstrasse 4, D-3400 Gottingen, Germany, 1993.
- [23] *International Tables for Crystallography*; Kynoch Press: Birmingham, UK, 1974, Vol. C.
- [24] Fischer, H.; Triliomis, A.; Gerbing, U.; Huber, B.; Mueller, G. *J Chem Soc, Chem Commun* 1987, 559.
- [25] Fischer, H.; Gerbing, U.; Triliomis, A.; Mueller, G.; Huber, B.; Riede, J.; Hofmann, J.; Burger, P. *Chem Ber* 1988, 121, 2095.

- [26] Nakayama, J.; Mizumura, A.; Akiyama, I.; Nishio, T.; Iida, I. *Chem Lett* 1994, 77.
- [27] Murai, T.; Mizutani, T.; Kanda, T.; Kato, S. *Heteroat Chem* 1995, 6, 241.
- [28] Otten, P. A.; Gorter, S.; van der Gen, A. *Chem Ber* 1997, 130, 49.
- [29] Blau, H.; Grobe, J.; Le Van, D.; Krebs, B.; Lage, M. *Chem Ber* 1997, 130, 913.
- [30] Li, G. M.; Zingaro, R. A.; Segi, M.; Reibenspies, J. H.; Nakajima, T. *Organometallics* 1997, 16, 756.
- [31] Li, G. M.; Reibenspies, J. H.; Zingaro, R. A. *Heteroat Chem* 1998, 9, 57.
- [32] Murai, T.; Niwa, N.; Ezaka, T.; Kato, S. *J Org Chem* 1998, 63, 374.
- [33] Hope, H. *Acta Crystallogr* 1965, 18, 259.
- [34] Perez-Rodriguez, M.; Lopez-Castro, A. *Acta Crystallogr* 1969, B25, 532.
- [35] Rutherford, J. S.; Calvo, C. *Kristallogr Z* 1969, 128, 229.
- [36] Pauling, L. In: *The Nature of the Chemical Bond*, 3rd ed.; Cornell University Press: Ithaca, NY, 1960, Ch. 7, pp. 260–261.